

## **Reliability Assessment of NPC inverters in PV Systems Under Power Degradation and Over-Temperature Derating Operation**

Chen, Meng; Sangwongwanich, Ariya; Zhou, Dao; Blaabjerg, Frede

*Published in:*

2023 IEEE 14th International Symposium on Power Electronics for Distributed Generation Systems (PEDG)

*DOI (link to publication from Publisher):*

[10.1109/PEDG56097.2023.10215265](https://doi.org/10.1109/PEDG56097.2023.10215265)

*Creative Commons License*

CC BY-NC-ND 4.0

*Publication date:*

2023

*Document Version*

Accepted author manuscript, peer reviewed version

[Link to publication from Aalborg University](#)

*Citation for published version (APA):*

Chen, M., Sangwongwanich, A., Zhou, D., & Blaabjerg, F. (2023). Reliability Assessment of NPC inverters in PV Systems Under Power Degradation and Over-Temperature Derating Operation. In *2023 IEEE 14th International Symposium on Power Electronics for Distributed Generation Systems (PEDG)* (pp. 54-60). Article 10215265 <https://doi.org/10.1109/PEDG56097.2023.10215265>

### **General rights**

Copyright and moral rights for the publications made accessible in the public portal are retained by the authors and/or other copyright owners and it is a condition of accessing publications that users recognise and abide by the legal requirements associated with these rights.

- Users may download and print one copy of any publication from the public portal for the purpose of private study or research.
- You may not further distribute the material or use it for any profit-making activity or commercial gain
- You may freely distribute the URL identifying the publication in the public portal -

### **Take down policy**

If you believe that this document breaches copyright please contact us at [vbn@aub.aau.dk](mailto:vbn@aub.aau.dk) providing details, and we will remove access to the work immediately and investigate your claim.



# Reliability Assessment of NPC inverters in PV Systems Under Power Degradation and Over-Temperature Derating Operation

Meng Chen, Ariya Sangwongwanich, Dao Zhou, and Frede Blaabjerg

AAU Energy  
Aalborg University  
Aalborg, Denmark

mche@energy.aau.dk, ars@energy.aau.dk, zda@energy.aau.dk, fbl@energy.aau.dk

**Abstract**—This paper presents an assessment of the reliability of neutral point clamped (NPC) based photovoltaic (PV) systems using a mission profile. The study focuses on the two types of fragile components in these systems, namely the insulated-gate bipolar transistors (IGBTs) and the DC Al electrolytic capacitors. Additionally, the effects of power degradation due to the aging of PV panel and the over-temperature derating characteristics of the NPC inverter are considered to make the lifetime evaluation more realistic. The evaluation is demonstrated using a study case of a 225 kW PV system based on actual mission profile and commercial components. The study results indicate that careful consideration of these factors is crucial to improve the design and operation of NPC inverter-based PV systems. This paper provides valuable insights into the evaluation of the reliability of NPC inverter-based PV systems.

**Index Terms**—PV systems, neutral point clamped inverter, reliability, power degradation, over-temperature derating

## I. INTRODUCTION

Photovoltaic (PV) systems are widely used for renewable energy generation and are usually connected to power systems via inverter that consist of semiconductor devices such as insulated-gate bipolar transistors (IGBTs) and diodes. The long-term reliability of these components is directly related to the mission profile, which includes ambient temperature ( $T_a$ ) and solar irradiance ( $S$ ) for PV systems [1]. Among these components, IGBTs are known to be fragile and have a larger impact on the reliability of PV systems compared to diodes. Previous studies have evaluated the reliability of PV systems at the IGBT and/or inverter level based on long-term mission profiles and various power strategies [2], [3].

However, in practical applications, the annual power attenuation of PV panels lead to an actual lifetime of the PV inverter that can be more than twice the number obtained without considering power degradation [4]. The aforementioned works study the typical three-phase two-level inverter. Furthermore, the neutral point clamped (NPC) three-level inverter is increasingly used for integrating renewable energy sources (RESs)

into large power systems due to its smaller harmonics [5]. The thermal stresses on different IGBTs of an NPC inverter are not identical, and the outer IGBTs are usually recognized as fragile due to larger switching losses, leading to differences between the two-level inverter and the NPC inverter when performing reliability analyses.

Another fragile component of inverter systems is the DC Al electrolytic capacitor (DC-Al-Cap), which has received increasing attention in recent years. Until now, the reliability of the DC-Al-Caps has been evaluated under various applications, e.g., wind power system, PV system, and multiple drives system [6]–[8]. Unlike IGBTs, the main failure mechanism of DC-Al-Caps is electrolyte loss due to thermal stress. Although the reliability of IGBTs and DC-Al-Caps can be separately analyzed, factors influencing their lifetimes can be the same due to the fact that their failures are out of the power loss and thermal stress [9], [10]. Therefore, panel degradation can also significantly affect the lifetime of DC-Al-Caps in PV systems.

To optimize renewable energy utilization, maximum power point tracking such as based on perturbation and observation (P&O MPPT) control is widely used in PV systems [11]. Although a rated power limitation of the inverter is considered in reliability analyses to avoid excessive thermal stress, it is not typically used in practice. Instead, a commercial semiconductor module recommends changing its power limitation according to the ambient temperature, also known as the over-temperature derating (OTD) curve. A low  $T_a$  allows the PV system to output more power than its rated value, whereas a high  $T_a$  requires derating operation [12]. The application of OTD curves can significantly change the thermal stress in practice and thus affect the reliability of PV systems.

Therefore, this paper proposes a reliability assessment of NPC inverter-based PV systems that focuses on both IGBTs and DC-Al-Caps. The paper also considers the effects of power degradation due to panel aging and the OTD characteristics of the inverter, and provides a case study of a 225 kW PV system based on actual mission profiles and commercial components.

This work was supported by the Reliable Power Electronic-Based Power System (REPEPS) project at the Department of Energy Technology, Aalborg University as part of the Villum Investigator Program funded by the Villum Foundation.

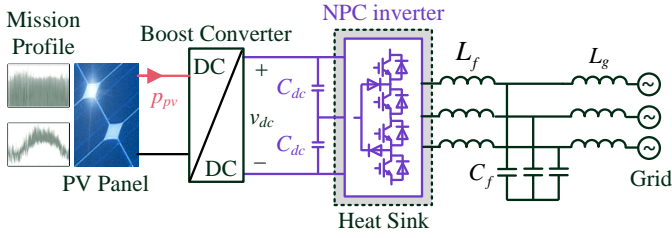


Fig. 1. General configuration of NPC inverter-based PV system.

TABLE I  
PARAMETERS OF NPC INVERTER-BASED PV SYSTEM

Symbol	Description	Value
$P_n$	Nominal power	225 kW
$f_{sw}$	Switching frequency	16 kHz
$\omega_g$	Grid frequency	$100\pi$ rad/s
$V_g$	Line-to-line RMS grid voltage	800 V
$L_g$	Grid-side inductor	0.0135 mH
$C_f$	Filter capacitor	100 $\mu$ F
$L_f$	Inverter-side inductor	0.185 mH
$C_{dc}$	DC capacitor	4000 $\mu$ F
$v_{dc}$	DC voltage	1300 V

## II. OVERVIEW OF STUDIED PV CASE

### A. System Description

Fig. 1 shows the general configuration of an NPC inverter-based PV system. The three-phase NPC inverter-based PV system is connected to the power grid via an LCL filter, where  $L_f$  and  $L_g$  are the inverter-side and grid-side filter inductors, respectively, and  $C_f$  is the filter capacitor. The main parameters are listed in Table I. The thermal stress and then the reliability of the inverter system is directly related to the power derived from the PV panel, i.e.,  $p_{pv}$ , which is determined by the mission profile, control strategy, etc., and will be analyzed in Section II-B.

The PV panel consists of 24 modules in parallel and 28 in series, where the LR4-72HPH 440M PV module from Longi Solar is used [13]. Similarly, the DC-Al-Cap  $C_{dc}$  in Fig. 1 actually consists of 12 capacitors in parallel and 2 capacitors in series of commercial capacitors. For the NPC inverter, a commercial module is used, where the topology is shown in Fig. 2. As mentioned before, the thermal stresses on different IGBTs of an NPC inverter are different. As a result, the outer IGBTs T1/T4 and the inner IGBTs T2/T3 are chosen with different types as well in the commercial module. In Fig. 2, the tested switching loss of T1/T4 in a standard condition (not the mission profile condition) is much smaller than that of T2/T3. At last, the thermal resistance of the heatsink is measured as  $0.021$   $^{\circ}\text{C}/\text{W}$  so that its temperature is around  $82$   $^{\circ}\text{C}$  when  $T_a = 40$   $^{\circ}\text{C}$  and the PV panel outputs the rated power.

### B. Analysis on Power Derived from PV panel

The thermal stress of the inverter is directly influenced by the PV power  $p_{pv}$ , which can be analyzed based on Fig. 3. Usually, the MPPT control is used to let the PV panel output its

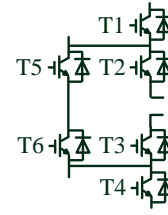


Fig. 2. Topology of used module of NPC inverter.

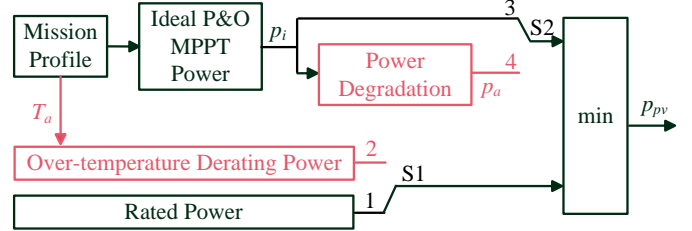


Fig. 3. Power derived from PV panel.

maximum power based on the mission profile. In most studies, the PV panel is modeled in such a way that an ideal maximum power  $p_i$  will be derived. Meanwhile, the rated power can be set as the upper limitation of  $p_{pv}$  to deviate the operation point away from the MPPT point, which can prevent an over-loaded operation of the inverter, i.e., S1 and S2 switch to 1 and 3 in Fig. 3, respectively. However, this strategy may not represent the operation of the PV system in practice.

The rated power is defined at a specific operation environment (e.g.,  $T_a = 40$   $^{\circ}\text{C}$ ). An OTD characteristics is actually used for the studied commercial PV system, as shown in Fig. 4, to achieve a better economic benefit. As observed, the PV inverter is allowed to operate with as much as  $(10/9)P_n$  when  $T_a$  is low to fully utilize the capacity. On the contrary, for a large  $T_a$ , the output power should be decreased from  $P_n$  due to the fact that a large thermal stress will shorten the lifetime of the inverter although the electrical stress is still within the limitation. When considering the OTD characteristics, S1 should be switched to 2 to derive  $p_{pv}$  in Fig. 3. The mission profile plays an important role when considering the OTD characteristics. In this paper, a realistic yearly mission profile with a resolution of 1 min/sample in Middle East is used as shown in Fig. 5. As observed, during the summer, the maximum temperature is liable to be larger than  $40$   $^{\circ}\text{C}$ , where the PV inverter should be with the derating operation. On the contrary, an overrating operation is permitted during the other months of the year.

Another factor which can influence  $p_{pv}$  is the panel degradation. For the studied LR4-72HPH 440M PV module, the standard degradation characteristics is shown in Fig. 6, which implies a 2% degradation for the first year and 0.55% for the following years. For example, the output power of the PV panel after operating 10 years will decrease to 93.05% compared to a new one. Therefore, the actual maximum power from the PV panel is not  $p_i$  but  $p_a$  as shown in Fig. 3.

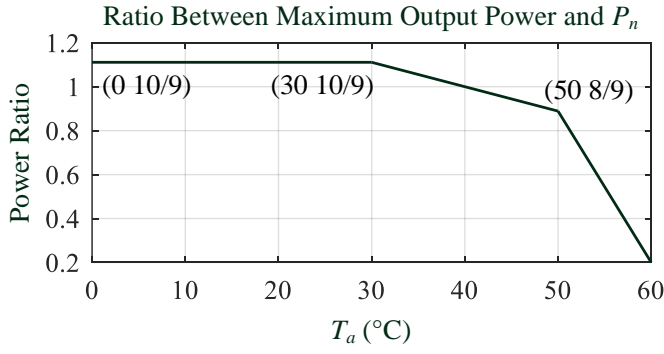


Fig. 4. Over-temperature derating (OTD) characteristics.

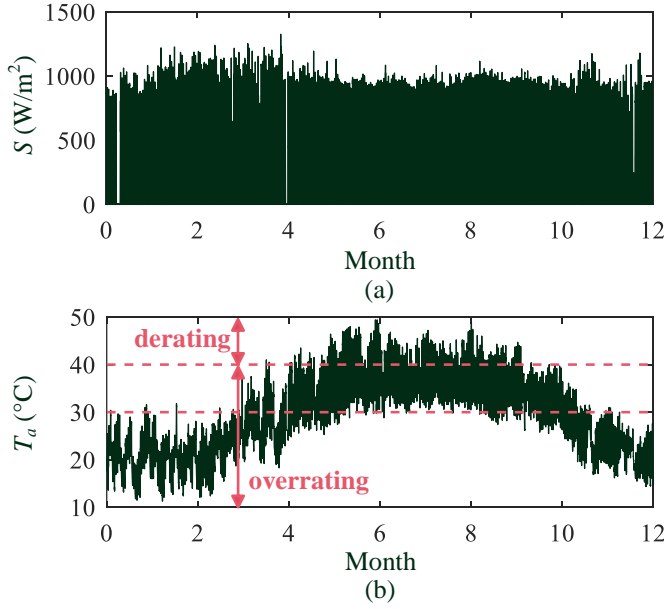


Fig. 5. Used yearly mission profile in Middle East. (a) Solar irradiance. (b) Ambient temperature.

Although the actual degradation rate may be changed due to the environment, Fig. 6 can be used to illustrate the influence of the panel degradation on the reliability of the PV inverter, which corresponding to the position 4 for S2 in Fig. 3.

According to the positions of S1 and S2, four cases as shown in Table II are studied and compared in this paper. Fig. 7 shows the differences of  $p_{pv}$  with or without considering the OTD and panel degradation (10 years of degradation is used as an example) characteristics. It clearly shows that the PV panel cannot output  $P_n$  during the summer due to a derating operation, which in winter, a larger  $p_{pv}$  than  $P_n$  can be expected. Meanwhile, when considering a 10 years panel degradation, the actual  $p_{pv}$  will decrease compared to a new one. The differences in  $p_{pv}$  may have obvious impact on the thermal stress and then the reliability of the PV inverter.

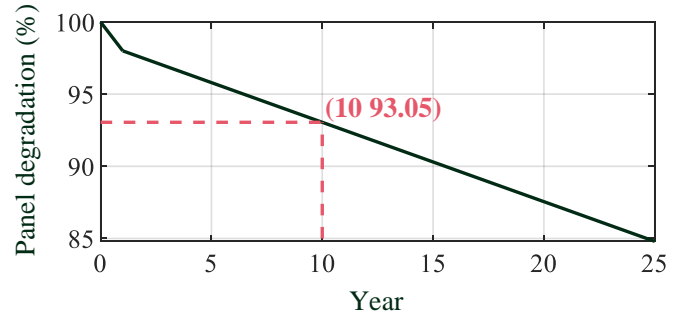


Fig. 6. Standard panel degradation characteristics of LR4-72HPH 440M PV module.

TABLE II  
STUDIED CASES

	Case 1	Case 2	Case 3	Case 4
S1	1	1	2	2
S2	3	4	3	4

### III. MISSION PROFILE-BASED LIFETIME EVALUATION

#### A. Overview Procedure

The power derived from the PV panel  $p_{pv}$  based on the mission profile can be further used to obtain the thermal loading and then to evaluate the lifetime of the inverter. The procedure can be illustrated by the flowchart in Fig. 8.

For IGBTs, the thermal stress is related to the power loss (including both of the conduction loss and the switching loss). With the derived mission profile-based  $p_{pv}$  in Fig. 7,  $p_{loss}$  of the IGBT can be obtained, e.g., by the look-up table method. Afterwards, the junction temperature of the IGBT  $T_j$  can be calculated based on the thermal model, where, for the studied module, the thermal model of the IGBT is modeled by a fourth-order Foster RC network. Then a rainflow counting analysis is carried out to identify the cycles information of the irregular mission profile-based  $T_j$ , i.e., junction temperature fluctuation  $\Delta T_j$ , mean junction temperature  $T_{jm}$ , heat time of the power cycling  $t_{on}$ , and the number of cycles  $n_i$ . At last, the number of cycles to failure of the IGBT  $N_f$  can be calculated by the lifetime model and then the accumulated damage  $AD_{IGBT}$  can be derived, which will be explained in the following.

For DC-Al-Caps, the thermal stress is also related to the power loss as the IGBTs. Nevertheless, the power loss of the DC-Al-Caps should be calculated based on the frequency-dependent ripple currents  $I_x$ , which will cause a heating temperature by  $\Delta T$ . Thereafter, the hours to failure  $L_x$  can be evaluated and the accumulated damage  $AD_{CAP}$  can be derived.

#### B. Lifetime Evaluation of IGBTs

The failure of the IGBT is related to its junction temperature. Specifically, the number of cycles to failure  $N_f$  can be

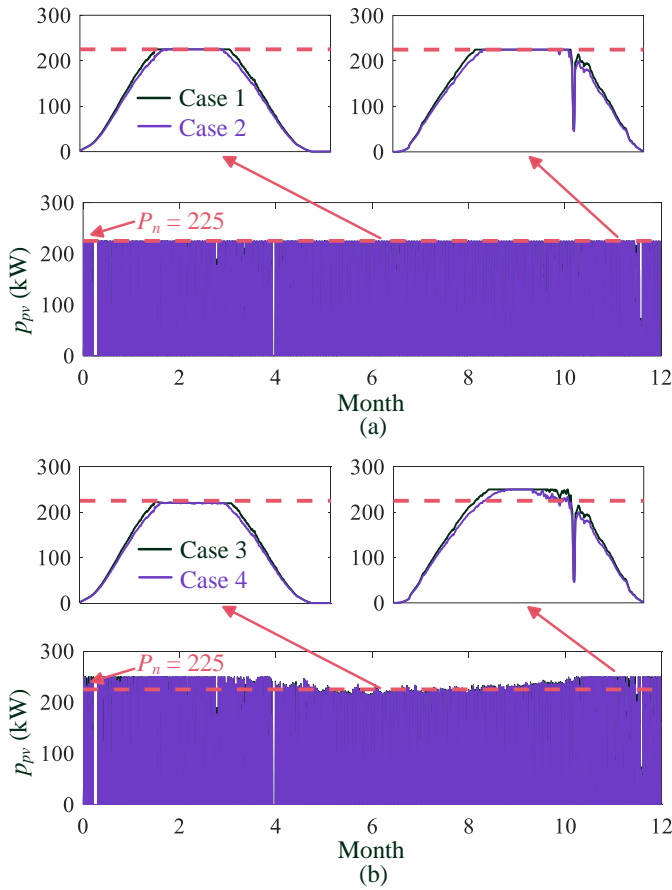


Fig. 7. Comparisons on power derived from PV panel. (a) Case 1 and Case 2. (b) Case 3 and Case 4.

TABLE III  
PARAMETERS OF LIFETIME MODEL OF IGBTs

Symbol	Value	Symbol	Value
$A$	$3.37 \times 10^{+0}$	$\beta$	$3.12 \times 10^3$
$\alpha$	-4.85	$\gamma$	-0.3

predicted by [2], [4]

$$N_f = A(\Delta T_j)^\alpha \exp\left(\frac{\beta}{T_{jm}}\right) \left(\frac{t_{on}}{1.5}\right)^\gamma \quad (1)$$

where  $A$ ,  $\alpha$ ,  $\beta$ , and  $\gamma$  are parameters, which are derived using a curve fitting method and are listed in Table III. As the minimum  $t_{on}$  is 60 s, which equals the resolution of the mission profile, the viscoplastic deformation saturation is also considered.

Thereafter, the mission profile-based  $AD_{IGBT}$  can be derived according to the Miner's rule, by placing the rainflow counting results into (1), as

$$AD_{IGBT} = \sum_i \frac{n_i}{N_{fi}} \quad (2)$$

Fig. 9(a) compares the results of T1/T4 with and without the OTD and panel degradation characteristics. For case 1, the

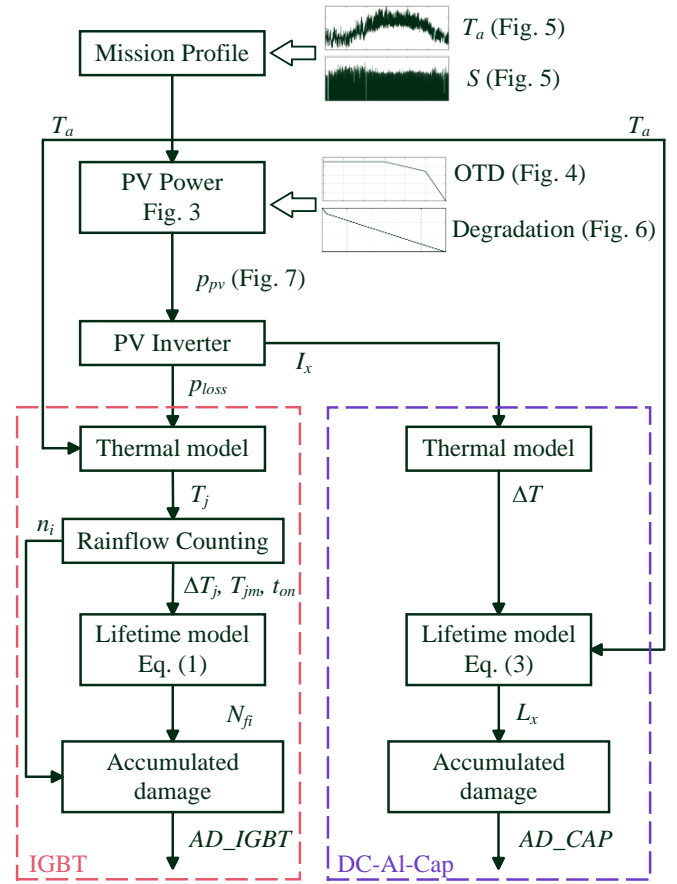


Fig. 8. Flowchart of lifetime evaluation for IGBT and DC-Al-Cap.

lifetime of T1/T4 is predicted to be 31.9 years. When taking the panel. When taking the panel degradation, i.e., Case 2, and OTD characteristics, i.e., Case 3, into consideration, the lifetime increases to 33.4 years and decreases to 22.8 years, respectively, where the number is 24.1 years when both of them are considered. The maximum difference, between Case 2 and Case 3, could be nearly 11 years for the studied system.

### C. Lifetime Evaluation of DC-Al-Cap

The failure of the DC-Al-Cap is related to two factors, one of which is the thermal stress due to the ambient temperature, and the other one is the heating temperature due to the ripple currents. Therefore, the hours to failure  $L_x$  can be predicted by [6], [7]

$$L_x = L_o \times 2^{(T_o - T_a)/10} \times 2^{(\Delta T_o - \Delta T)/p_1} \quad (3)$$

where  $L_o$  is the rated useful lifetime,  $T_o$  is the upper categorized temperature,  $\Delta T_o$  is the heating temperature at rated ripple current,  $p_1$  is the coefficient of temperature rise. For the studied capacitor, the corresponding parameters are listed in Table IV.

Fig. 9(b) compares the results of DC-Al-Cap for different cases. The lifetime prediction gives a result of 40.8 years for Case 1, 48 years for Case 2, and 37.9 years for Case 3. When

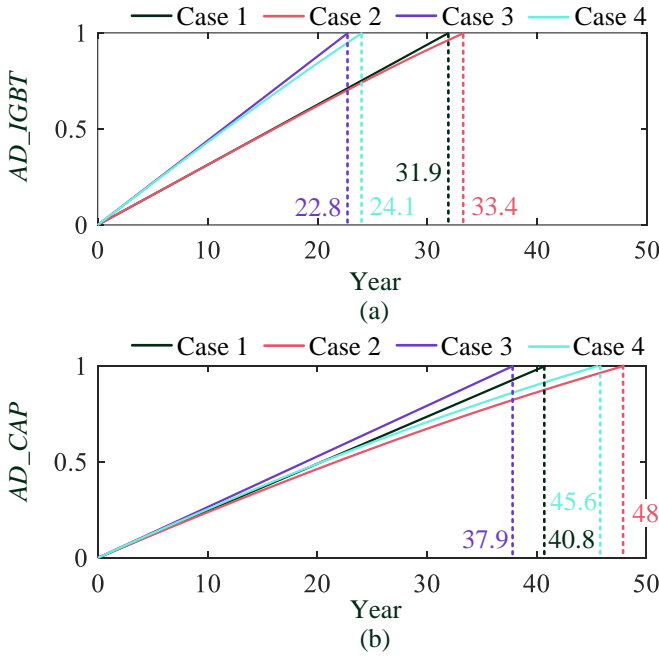


Fig. 9. Accumulated damage of (a) T1/T4 and (b) DC-Al-Cap.

TABLE IV  
PARAMETERS OF LIFETIME MODEL OF DC-AL-CAP

Symbol	Description	Value
$L_o$	Rated useful lifetime	5000 h
$T_o$	Upper categorized temperature	105 °C
$\Delta T_o$	Heating temperature at rated ripple current	5 °C
$p_1$	Coefficient of temperature	5

taking both of the panel degradation and OTD characteristics into consideration, the lifetime is expected to be 45.6 years. Meanwhile, the maximum difference, between Case 2 and Case 3, is 10 years for the studied system.

By combining the results of Fig. 9, it is noticed that the impact of panel degradation and OTD characteristics on T1/T4 and DC-Al-Cap may be different. For T1/T4, the OTD characteristics have more obvious influence. For example, from Case 1 to Case 3, the lifetime decreases by 28.5% due to the OTD characteristics, while to Case 2, the lifetime changes by only 4.7% affected by the panel degradation. On the contrary, the DC-Al-Cap is more sensitive to the panel degradation, where the lifetime increases by 17.6% from Case 1 to Case 2. However, with considering the OTD characteristics, the lifetime of DC-Al-Cap changes by only 7.1% from Case 1 to Case 3.

#### IV. RELIABILITY ASSESSMENT BASED ON MONTE CARLO ANALYSIS

Compared to the aforementioned fix-parameter lifetime evaluation, a more realistic reliability assessment should consider the variations of parameters. To do so, this section utilize the Monte Carlo analysis to perform a statistical study, where the procedure is illustrated by the flowchart in Fig. 10.

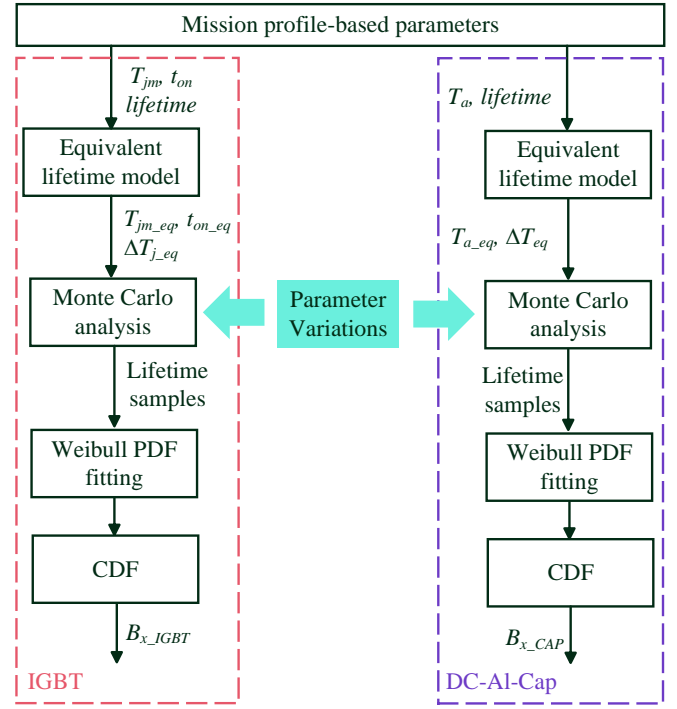


Fig. 10. Flowchart of reliability assessment based on Monte Carlo Analysis.

In Section III, the mission profile-based parameters have been obtained. To perform the Monte Carlo analysis, those parameters are, at first, translated into corresponding equivalent static parameters (for IGBT, they are denoted as  $T_{jm\_eq}$ ,  $t_{on\_eq}$ ,  $\Delta T_{j\_eq}$ , and for DC-Al-Cap denoting as  $T_{a\_eq}$ ,  $\Delta T_{eq}$ ) in such a way that the lifetimes of IGBT and DC-Al-Cap derived from the equivalent parameters equal to those mission profile-based results. Thereafter, the Monte Carlo analysis is carried out by considering  $\pm 5\%$  parameter variations and 10000 samples. For the lifetime model of IGBT in (1), all the parameters  $A$ ,  $\alpha$ ,  $\beta$ ,  $\gamma$  as well as the equivalent parameters  $T_{jm\_eq}$ ,  $t_{on\_eq}$ ,  $\Delta T_{j\_eq}$  are supposed to be variable. Similarly, the variations of  $L_o$ ,  $T_o$ ,  $\Delta T_o$ ,  $p_1$ ,  $T_{a\_eq}$  and  $\Delta T_{eq}$  are all considered for the DC-Al-Cap. The derived lifetime samples from the Monte Carlo analysis can be fitted by the Weibull probability density function (PDF), based on which the cumulative density function (CDF) can be further derived. Finally, the  $B_x$  lifetime can be found on the CDF, which reflects the unreliability level of the corresponding components and systems.

Fig. 11 shows the CDFs for both T1/T4 and DC-Al-Cap with the same four cases as Table II, where the usually used  $B_{10}$  lifetimes are marked as well. For T1/T4, the expected time of Case 1 that the unreliability increases to 10% is 15.8 years. When the panel degradation or/and OTD characteristics are included, corresponding from Case 2 to Case 4,  $B_{10\_IGBT}$  changes to 16.6, 11.5, and 12.1 years, respectively. It can be calculated that the maximum difference, i.e., between Case 2 and Case 3, is 5.1 years, which accounts for 44.4% taking Case 3 as the basis and 30.7% taking Case 2 as the basis.

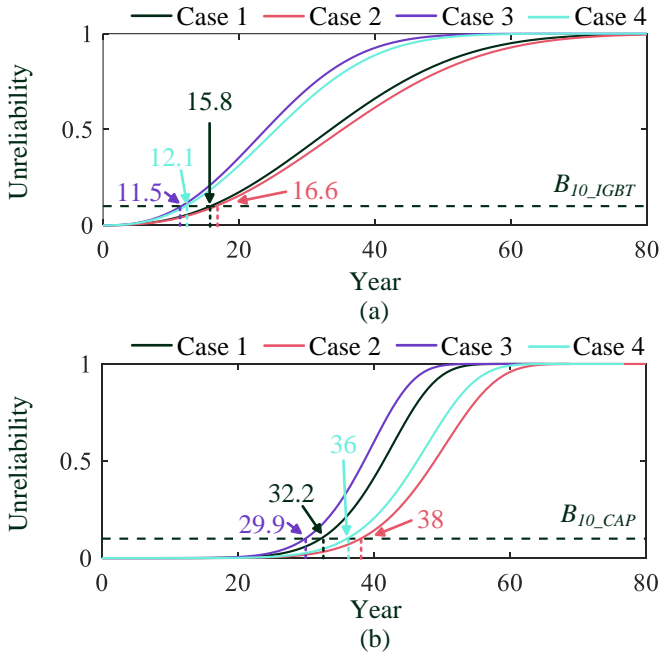


Fig. 11. Cumulative density function (CDF). (a) T1/T4. (b) DC-Al-Cap.

Similarly,  $B_{10\_CAP}$  is 32.2, 38, 29.9, and 36 years from Case 1 to Case 4, respectively. These numbers highlight the role of the panel degradation and OTD characteristics.

Fig. 11 is the CDF of a single component. In actual, the studied three-phase NPC inverter has 6 outer IGBTs as well as 48 DC-Al-Caps as described in Section II-A, where the damage of any of them will make the whole system to be out of function. Therefore, the system-level CDFs of IGBT and DC-Al-Cap can be calculated, respectively, by

$$CDF_{sys\_IGBT} = 1 - (1 - CDF_{IGBT})^6 \quad (4)$$

$$CDF_{sys\_CAP} = 1 - (1 - CDF_{CAP})^{48} \quad (5)$$

where  $CDF_{IGBT}$  and  $CDF_{CAP}$  are CDFs of the corresponding single component in Fig. 11. Fig. 12 presents the derived system-level CDFs, where  $B_{10\_sys\_IGBT}$  and  $B_{10\_sys\_CAP}$  values are decreased to between 5 and 25 years compared to the values of single component. Again, the results prove that the panel degradation and OTD characteristics could have important impact on the reliability of the NPC inverter-based PV system.

It should be mentioned that the actual results could be very different for different systems and mission profiles. For example, as shown in Fig. 5, there is a complementarity on the lifetime between the derating and overrating operation with the used mission profile. However, it is highly dependent on the locations, where, such as in Denmark, there is almost no derating operations and the lifetime is expected to be highly decreased by the overrating operation. Nevertheless, the results prove, in general, that the panel degradation and OTD characteristics could have important impact on the lifetime

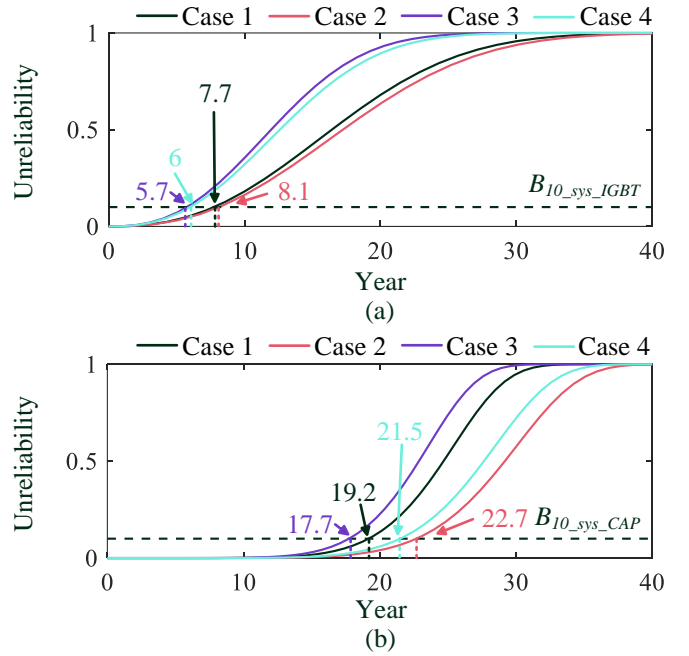


Fig. 12. System-level CDFs. (a) Outer IGBTs. (b) DC-Al-Cap.

evaluation of the PV system, which can be analyzed by using Fig. 3.

## V. CONCLUSION

This paper presents a reliability assessment on NPC inverter-based PV systems using commercial components and actual mission profile. The impact of panel degradation and OTD characteristics on the fragile components, i.e., the outer IGBT and DC-Al-Cap, has been considered. The analysis reveals that the reliability of the PV system can be quite different with and without taking the panel degradation and OTD characteristics into account. Therefore, it is recommended including them into the PV system design during the early stage.

## REFERENCES

- [1] A. F. Cupertino, J. M. Lenz, E. M. Brito, H. A. Pereira, J. R. Pinheiro, and S. I. Seleme, "Impact of the mission profile length on lifetime prediction of PV inverters," *Microelectron. Reliab.*, vol. 100-101, pp. 1–6, Sep. 2019.
- [2] P. D. Reigosa, H. Wang, Y. Yang, and F. Blaabjerg, "Prediction of bond wire fatigue of IGBTs in a PV inverter under a long-term operation," *IEEE Trans. Power Electron.*, vol. 31, no. 10, pp. 7171–7182, 2015.
- [3] R. D. P. Silva, D. B. da Silveira, R. C. de Barros, J. M. S. Callegari, A. F. Cupertino, and H. A. Pereira, "Third-harmonic current injection for wear-out reduction in single-phase PV inverters," *IEEE Trans. Energy Convers.*, vol. 37, no. 1, pp. 120–131, Mar. 2022.
- [4] A. Sangwongwanich, Y. Yang, D. Sera, and F. Blaabjerg, "Lifetime evaluation of grid-connected PV inverters considering panel degradation rates and installation sites," *IEEE Trans. Power Electron.*, vol. 33, no. 2, pp. 1225–1236, Feb. 2018.
- [5] V. Yaramasu and B. Wu, "Predictive control of a three-level boost converter and an NPC inverter for high-power PMSG-based medium voltage wind energy conversion systems," *IEEE Trans. Power Electron.*, vol. 29, no. 10, pp. 5308–5322, Oct. 2014.

- [6] D. Zhou, Y. Song, Y. Liu, and F. Blaabjerg, "Mission profile based reliability evaluation of capacitor banks in wind power converters," *IEEE Trans. Power Electron.*, vol. 34, no. 5, pp. 4665–4677, May 2019.
- [7] D. Zhou and F. Blaabjerg, "Converter-level reliability of wind turbine with low sample rate mission profile," *IEEE Trans. Ind. Appl.*, vol. 56, no. 3, pp. 2938–2944, May 2020.
- [8] H. Wang, S. Huang, D. Kumar, Q. Wang, X. Deng, G. Zhu, and H. Wang, "Lifetime prediction of DC-link capacitors in multiple drives system based on simplified analytical modeling," *IEEE Trans. Power Electron.*, vol. 36, no. 1, pp. 844–860, Jan. 2021.
- [9] Y.-J. Kim, S.-M. Kim, and K.-B. Lee, "Improving DC-link capacitor lifetime for three-level photovoltaic hybrid active NPC inverters in full modulation index range," *IEEE Trans. Power Electron.*, vol. 36, no. 5, pp. 5250–5261, May 2021.
- [10] A. Das, Y. Gupta, S. Anand, and S. R. Sahoo, "Temperature droop-based dynamic reactive power sharing technique to improve the lifetime of power electronic converter," *IEEE Trans. Power Electron.*, vol. 37, no. 5, pp. 5245–5255, May 2022.
- [11] J. P. Ram, T. S. Babu, and N. Rajasekar, "A comprehensive review on solar PV maximum power point tracking techniques," *Renew. Sustain. Energy Rev.*, vol. 67, pp. 826–847, Jan. 2017.
- [12] I. Vernica, K. Ma, and F. Blaabjerg, "Optimal derating strategy of power electronics converter for maximum wind energy production with lifetime information of power devices," *IEEE J. Emerg. Sel. Top. Power Electron.*, vol. 6, no. 1, pp. 267–276, Mar. 2018.
- [13] *High Efficiency Low LID Mono PERC with Half-cut Technology*, LR4-72HPH 420~440M, LONGi Solar, 2019.